European Journal of Environmental and Civil Engineering

Revue Française de Génie Civil

Volume 29 Number 13 November 2025

Taylor & Francis

ISSN: 1279-5119 (Print) Journal homepage: www.tandfonline.com/journals/tece18

Thermo-mechanical behaviour of soils

Lyesse Laloui

To cite this article: Lyesse Laloui (2001) Thermo-mechanical behaviour of soils, Revue Française de Génie Civil, 5:6, 809-843, DOI: 10.1080/12795119.2001.9692328

To link to this article: https://doi.org/10.1080/12795119.2001.9692328

Thermo-mechanical behaviour of soils

Lyesse Laloui

Soil Mechanics Laboratory
Swiss Federal Institute of Technology, Lausanne
CH-1015 Lausanne, Switzerland

Lyesse.Laloui@epfl.ch

ABSTRACT. Research interest in the thermo-mechanical behaviour of soils is growing as a result of an increasing number of geomechanical problems involving thermal effects. It is, therefore, necessary to understand thermally induced effects on soils and then to use the appropriate constitutive models for the numerical simulation of such phenomena. This paper addresses various issues concerning the thermo-mechanical behaviour of soils. Starting from experimental evidence of non-linearity and hardening that heating causes in soils, thermodynamic considerations are then introduced for the derivation and the discussion of the general form of the constitutive equations. After that, constitutive modelling is presented and treated in the context of elasto-plasticity based on the LTVP model, which includes the evolution of yield surfaces with temperature. Numerical simulations support the theoretical aspects of the paper by showing performances of this constitutive law, especially for undrained and cyclic paths.

KEYWORDS: Constitutive modelling, elasto-thermoplasticity, thermodynamics, thermal effects.

RFGC – 5/2001. Environmental Geomechanics, pages 809 to 843

1. Introduction

In recent years, thermal geomechanical problems have increased enormously as a result of the demand for new and increased types of applications. There are many applications based on the understanding of the thermo-mechanical behaviour of soils, notably for high-level nuclear waste disposal [LAL 94], heat storage [BUR 85], geothermal structures [LAL 99], petroleum drilling, injection and production activity [DUS 88], zones around buried high-voltage cables [MIT 82] and others related to the seasonal and daily cyclical changes of temperature such as road subgrades, furnace foundations, and sample disturbance due to temperature changes during sampling, storage and testing. Due to the importance of such applications, the thermo-mechanical behaviour of soils is becoming one of the major issues in modern soil mechanics. Several of the leading research teams around the world have now implemented research programmes in this area.

The topics' development in the thermo-mechanical area concern:

– New testing and measuring devices dedicated to thermo-mechanical characterisation;

– Understanding of the thermo-mechanical behaviour of soils;

– Constitutive modelling;

– The introduction of constitutive laws inside thermo-hydro-mechanical (THM) formulations and the application to boundary value problems.

The challenges are great in all of the above-mentioned categories and significant advances have been made in recent years. Laboratory experiments are more complex than those for conventional Soil Mechanics. One additional field variable must be managed (temperature), which requires special techniques. Experimental evidence reveals the complex thermo-mechanical response of soils. As an example, the volumetric strain during heating is contractive for normally consolidated clays and a significant part of this strain is irreversible upon cooling. This thermal contraction is an unusual behaviour for any material. The existing thermo-plastic constitutive models must incorporate several missing aspects more adequately. Finally, the implementation of thermo-plastic models in THM finite element programs requires specific numerical techniques to treat the fully-coupled, non-linear and transient nature of the system of equations.

This paper addresses certain aspects of the thermo-mechanical constitutive modelling issue (stress-strain-temperature relations); it obviously does not pretend to be a state-of-the-art report on the subject. The aim is simply to present some significant results in this field. The layout is as follows: first, the principal experimental observations of the thermally induced effects on soils are shown in the light of the elasto-thermoplastic constitutive formulations. Starting from general considerations based on thermodynamics that permit the derivation and the discussion of the general form of the constitutive equations, a thermo-mechanical

framework is then introduced in Section 3. Thermo-mechanical modelling of soils is illustrated using an elasto-thermoplastic constitutive law (LTVP model). Finally, in Section 5, some selected comparisons between model simulations and experimental results for different combinations of thermo-mechanical loading paths are presented.

Here, the considered temperature range is from 4 °C to 95 °C, which corresponds to that of the principal geo-environmental applications concerned (without freezing or boiling of the pore water). This paper investigates the state of stress and strain in soils due to heating, under the simplifying assumption that the influence of strain on the temperature field may be neglected.

2. Principal experimental observations concerning thermally induced effects

There are numerous experimental results available in the literature, which show the influence of temperature on the behaviour of soils. Some disparities exist in these results which can be attributed to the complexity of the nature of different soils. In this section, a brief presentation of the principal experimental observations concerning thermally induced effects on soils is given. To clarify the presentation, three types of loading paths will be distinguished: thermal (Path 1), isothermal-mechanical (Path 2) and thermo-mechanical (Path 3). Path 1 represents the behaviour of a soil subjected to a temperature variation (the difference between the present and initial or reference temperatures) at constant stress. Path 2 corresponds to mechanical loading at a given constant temperature. Finally, Path 3 includes both thermal and mechanical loading, however, not imposed simultaneously, in order to permit the differentiation of their effects.

2.1. *Thermal behaviour (Path 1)*

Saturated soil is a two-phase material including a solid part (a skeleton of grains or particles surrounded by adsorbed water, for clays) and a fluid part (free water) in the inter-aggregate space (or voids). When a soil is heated, all of the constituents dilate. In the case of clayey soils, this dilation produces a decrease in the strength of the adsorbed layers and a modification in the distance between the clay particles [FLE 79], [ROB 96]. This changes the equilibrium between the Van der Waals attractive forces and the electrostatic repulsive forces, which results in one of the most characteristic thermal behaviours of clays. In normally consolidated conditions (NC), where the effect of stress is less important (than in overconsolidated conditions (OC)), the clay contracts when it is heated and a significant part of this deformation is irreversible upon cooling. This thermal contraction is an unusual behaviour for any material. Fig. 1 illustrates such results; the response to a thermal loading-unloading cycle at constant isotropic stress of a sample of saturated drained Illite is shown. The sample settles during heating with a non-linear volume variation.

During cooling, on the contrary, a relatively linear behaviour results in volume increase. The behaviour over the whole cycle indicates the irreversibility of strain due to thermal loading which is representative of thermal hardening. Even though there has been no physical change in effective stresses, this can be interpreted as the soil undergoing densification, i.e. overconsolidated behaviour. Thermal permanent deformation is also exhibited by overconsolidated soils [DEM 82]. The intensity of the reversible/irreversible parts of the deformation due to temperature cycling depends upon soil type and plasticity, in addition to stress level measured in terms of the overconsolidation ratio (OCR). This is illustrated in Fig. 2 where the influence of OCR on the thermal behaviour of several soils is shown. It can be noticed that, for a given increase in temperature, the compaction of a soil volume is smaller for higher overconsolidation ratios and then tends to dilation.

Another representation of the same behaviour of fine soils subjected to heating-cooling cycles is given in Fig. 3 [BAL 91]. After heating, NC clay contracts, while the OC state produces mainly reversible dilation. Between those states, an intermediate one (low OCR) first produces dilation, then a tendency toward contraction.

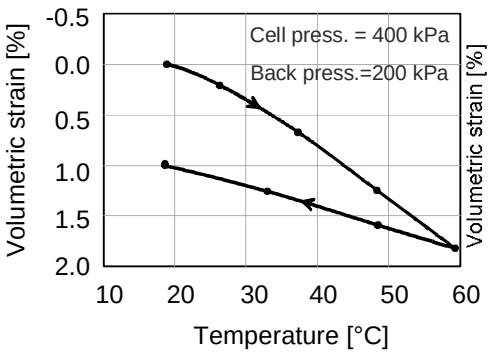

Figure 1. *Effects of temperature variation on a saturated Illite under constant isotropic compression [CAM 68]*

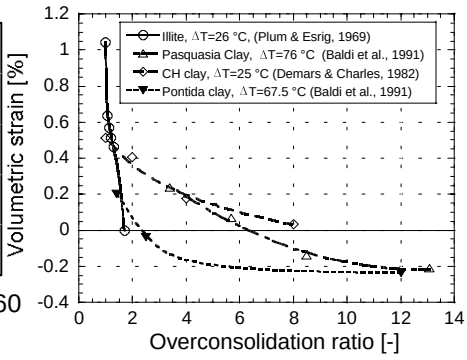

Figure 2. *Influence of over-consolidation ratio on the thermal strain of fine soils [CEK 01]*

2.2. *Mechanical behaviour (Path 2)*

Isotropic stress conditions

In the (*e*-ln *p*) plane, with *e* being the void ratio and *p* being the mean effective pressure, the slope of the consolidation line is independent of temperature. Experiments on saturated Illite at three different temperatures also show that heating applied prior to loading produces a densification of the sample at constant isotropic pressure (Fig. 4, [CAM 68]).

To analyse the change in the pre-consolidation pressure with respect to temperature, tests consist in heating the soil under stress loads smaller than the pre-consolidation value and then in applying mechanical load under a constant temperature.

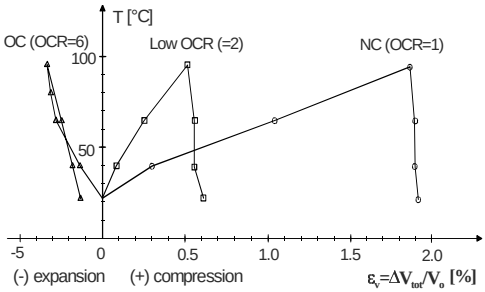

Figure 3. *Typical thermal behaviour of fine soils – Boom clay [BAL 91]*

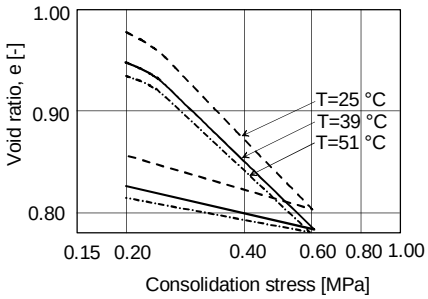

Figure 4. *Isotropic consolidation of Illite samples at three different temperatures [CAM 68]*

Fig. 5 illustrates such results for a pure clay [TIF 89], the clay of Bäckebol (Moritz, 1995) and a silty clay [ERI 89]. The pre-consolidation pressure decreases non-linearly with increased temperature. This decrease means that the yield limits in an isotropic plane decrease with temperature increase. This phenomenon is independent of viscous effects, as was shown by [BOU 94].

Deviatoric stress conditions

Until recently, the thermal effect on strength remained to be confirmed. Some researchers concluded that heating caused decrease in strength, while others reported slightly increased strength. Some experimental results are summarised in Fig. 6. This confirms that the friction angle at critical state can either increase or decrease (or remain independent) with temperature. In some cases, thermal dependency can be quite pronounced (Kaolin). It seems that the friction angle variation with temperature depends on the nature of the considered soil and it is more possible to obtain a decrease in this value through heating.

Thermal hardening induced by heating modifies density (or the critical pressure, in other words). This results in a different initial state at different temperatures. The combination of these two effects (friction angle and critical pressure variations) will produce shear strength dependency on temperature.

Undrained behaviour

When the free water cannot be drained out of the sample, the behaviour of the soil subjected to thermo-mechanical loading is strongly affected. Heating results in a significant pore pressure increase (ex. Newfields clay [PLUM 69], Fig. 7).

At a constant total stress difference, the pore pressure growth can induce failure in the sample. Experimental results on two clays reported by [HUE 89] have shown the failure of clays under undrained conditions at temperature values between 70°C to 90°C (Fig. 8 for Boom clay).

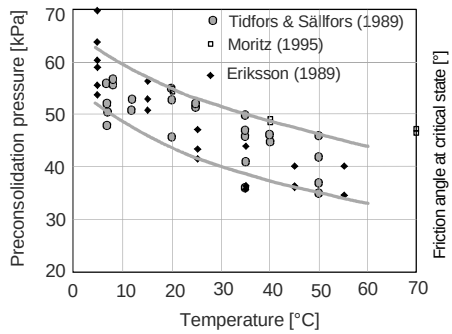

Figure 5. *Influence of temperature on pre-consolidation pressure [CEV 01]*

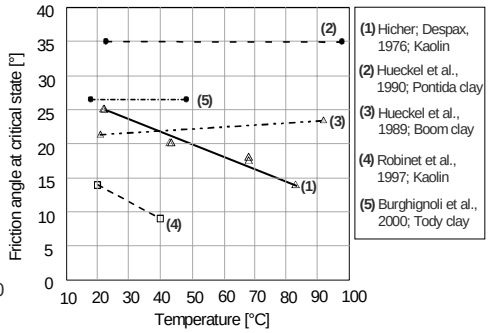

Figure 6. *Effect of temperature on friction angle at critical state [CEV 01]*

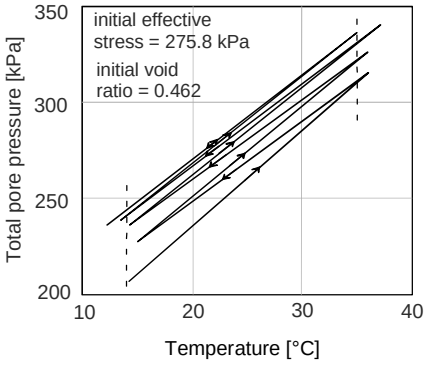

Figure 7. *Thermally induced pore pressure in undrained conditions of Newfield clay [PLU 69]*

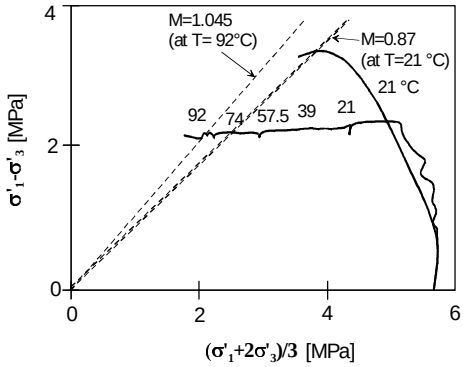

Figure 8. *Influence of temperature on the undrained behaviour of Boom clay [HUE 89]*

As it may be seen, this failure is due to an increase in pore pressure that leads to an effective main stress drop under constant total stress conditions until reaching the critical state line. The higher the initials deviatoric stress the faster the occurrence of failure.

3. Thermo-mechanical framework

An appropriate way to formulate thermo-mechanical constitutive models for soils rigorously is to assure their conformity with thermodynamics (in fact, thermostatics). Due to the complex behaviour of soils, one way to obtain this is to formulate the constitutive laws with conventional plasticity in accordance with experimental observations, and then to verify their conformity with the laws of thermodynamics retrospectively. The first part of this section is an introduction to such an approach. After that, a thermo-mechanical formulation based on the theory of plasticity is introduced.

3.1. *Application of thermodynamics to the derivation of a constitutive model*

The thermodynamic approach for describing the behaviour of deformable solids was stimulated in the 1950s, when Biot (1956) published several papers showing how the thermodynamics of irreversible processes, combined with mechanical theories, can provide the basis of a thermo-mechanical theory of viscoelasticity for infinitesimal deformation. [ZIE 75, 77, 87] derived an interesting method for describing material behaviour based on thermodynamics, including the non-associated flow rule. In particular, the fact that orthogonality in velocity space does not imply orthogonality in force space avoids the restrictions introduced by the theory of plastic potential. Discussions of this approach and some applications can be found in [HOU 81, 82] and [GER 83]. The thermodynamic basis underlying classical rate-independent plasticity within the framework of irreversible thermodynamics with internal state variables is not presented here, and only the equations resulting from their derivation are outlined below. Details on the mathematical derivations can be found in [LAL 93]. Thermodynamic considerations of hypoplastic constitutive models can be found in [SVE 99].

General assumptions and notations

A small deformation theory is assumed here, so that strains are described by the small strain tensor ε, and the deformation rate tensor is equal to its rate of change $\dot{\varepsilon}$. The state of the material is defined by ε, internal variables α (as the plastic strain) and temperature T.

3.1.1. *Thermodynamic formulation*

As shown above, the thermo-mechanical behaviour of soils includes some dissipative (plastic) processes. Thermodynamic considerations must include complementary laws related to these irreversibilities. These laws must be formulated with respect to the material indifference principle and the positivity of the dissipation function [HAL 75]. The second fundamental law of thermodynamics can be used for this purpose. The state function, which characterises the energy in the system, is the

specific free energy function $\psi(\varepsilon, \alpha, T)$, depending on state parameters (already defined in the general assumptions). The stress tensor σ is split into two parts [ZIE 75]: reversible (quasi-conservative) σ^r and irreversible (dissipative) σ^i, respectively:

$$\sigma^i = \sigma - \sigma^r \qquad [1]$$

The reversible part can be defined by the following relationship as the thermodynamic force associated with the strain tensor ε:

$$\sigma^r = \rho \partial_\varepsilon \psi \qquad [2]$$

With the specific dissipation function $\phi(T, \varepsilon, \alpha, \dot{\varepsilon}, \dot{\alpha}, \boldsymbol{q})$, the well-known Clausius-Duhem inequality can be written as:

$$\rho\phi = \sigma^i : \dot{\varepsilon} - \rho \partial_\alpha \psi : \dot{\alpha} - \frac{\boldsymbol{q}}{T} \cdot \nabla T \geq 0 \qquad [3]$$

with $\nabla = (\partial/\partial x, \partial/\partial y, \partial/\partial z)$, $(\sigma^i : \dot{\varepsilon})$ the $tr(\sigma^i \cdot \dot{\varepsilon})$, $\boldsymbol{q}$ the thermal flux and ρ the unit mass. As a small strain theory is assumed in this paper, the variations of ρ are neglected. While the free energy is a function of kinematic variables, the dissipation function is a function of kinematic variables, as well as of their rates of change [ZIE 77]. In the above relationship, each term is a product of a force and a velocity term. The irreversible stresses, thermal flux and internal dissipation terms characterise the irreversible process. Thus, the thermodynamic action (forces associated with the internal variables) is given as:

$$\vartheta = \rho \partial_\alpha \psi \qquad [4]$$

[ZIE 87] assume that the dissipation function can be written by means of a new function Φ* as:

$$\phi = \partial_{\dot{\varepsilon}} \Phi^* : \dot{\varepsilon} + \partial_{\dot{\alpha}} \Phi^* : \dot{\alpha} + \partial_{\boldsymbol{q}} \Phi^* . \boldsymbol{q} \geq 0 \qquad [5]$$

where Φ* is convex, continuous and non-negative. Comparing the above-mentioned Clausius-Duhem inequality and this equation, it is possible to define the first complementary law as the relationship between the irreversible stress tensor and Φ*:

$$\sigma^i = \rho \, \partial_{\dot{\varepsilon}} \Phi^* \qquad [6]$$

Similarly, the second complementary law (giving ϑ) and the thermal dissipating term can be found as:

$$\vartheta = -\rho\partial_{\dot{\alpha}}\,\Phi^* \quad ; \quad -\frac{1}{T}\cdot\nabla T = \rho\,\partial_{\boldsymbol{q}}\,\Phi^* \qquad [7]$$

The stress tensor is finally given by:

$$\sigma = \rho\partial_{\varepsilon}\psi + \rho\partial_{\dot{\varepsilon}}\,\Phi^* \qquad [8]$$

and the following consistency relationship for the thermodynamic forces ϑ is imposed to ψ and Φ^* :

$$\rho\partial_{\alpha}\psi + \rho\partial_{\dot{\alpha}}\,\Phi^* = 0 \qquad [9]$$

From these equations, the behaviour of a rate independent material can be completely determined, if the expressions of the free energy and the dissipation function are known (see [ZIE 87] for examples for standard constitutive models). This approach, which imposes some constraints for the choice of thermodynamically consistent evolution equations, is used here.

3.1.2. *Derivation of the constitutive model*

As shown above, it is possible to write the entire description of the thermo-mechanical behaviour based on the knowledge of two functions of kinematic variables: a thermodynamic potential, such as the Helmholtz free energy, and the dissipation function, if the latter is convex and non-negative. The constitutive model thus obtained respects the thermodynamic principle, which implies that the irreversible deformation generated by this model belongs to the space of admissible thermodynamic processes. The state and complementary laws being provided, the thermodynamic state can now be specified by the following state functions:

$$\psi\left(T,\varepsilon,\varepsilon^p\right) \quad \textit{and} \quad \Phi^*\left(T,\varepsilon,\varepsilon^p,\dot{\varepsilon},\dot{\varepsilon}^p\right)$$

in which we assume the internal state to be completely represented by the plastic strain. The defined state parameters are now able to decompose the free energy in three parts:

$$\psi = \psi_T\left(T\right) + \psi_{T\varepsilon}\left(T,\varepsilon\right) + \psi_{\varepsilon}\left(\varepsilon,\varepsilon^p\right) \qquad [10]$$

where the first one describes the thermal behaviour, the second one the thermo-mechanical coupling and the last one the mechanical behaviour.

As almost all constitutive models proposed in the literature for the thermo-mechanical modelling of soils belong to the Cam-clay family of models, the

thermodynamic basis of this model associated to the Roscoe dilatancy rule is presented here. This approach is then extended to an early version of the elasto-plastic model proposed by [HUJ 79], which will serve for the formulation of the elasto-thermoplastic model that will be introduced in Section 4.

Cam-clay model with the Roscoe dilatancy rule

The following expressions for free energy and dissipation functions may be written to describe a thermo-mechanical constitutive model assuming isotropic linear thermo-elasticity [LAL 93], [MOD 94]:

– free energy :

$$\rho\psi = \frac{1}{2}\left[A\theta^2 - 2\theta\beta_s' K\left(\varepsilon_v - \varepsilon_v^p\right) + K\left(\varepsilon_v - \varepsilon_v^p\right)^2 + 2G\left\|\mathbf{e} - \mathbf{e}^p\right\|^2 \right] \qquad [11]$$

– dissipation function :

$$\rho\Phi^* = -M\ p_c \left\|\dot{\mathbf{e}}^p\right\| \exp\left(\frac{-\dot{\varepsilon}_v^p}{M\left\|\dot{\mathbf{e}}^p\right\|} \right) \qquad [12]$$

with θ the temperature variation $\left(=T - T_0\right)$ with respect to an initial temperature T_0, K the bulk modulus, G the shear modulus, ε_v the volumetric strain $\left(=tr\,\varepsilon\right)$, $\mathbf{e}$ the deviatoric strain tensor $\left(\varepsilon - \frac{1}{3}\varepsilon_v \mathbf{I}\right)$, $\mathbf{I}$ the identity tensor, p_c the critical pressure $\left(= p_{co} \exp\left(-\beta\varepsilon_v^p\right)\right)$, p_{co} the initial critical pressure, β the plastic compressibility coefficient, β_s' the volumetric thermal expansion coefficient and M the slope of the critical state line in stress invariant $\left(p - q\right)$ space. "A" designates a thermal parameter, which will be defined below and $\|\ \|$ represents the norm of a tensor. The continuum mechanics sign convention is used here (i.e. traction is positive).

The selected Φ^* does not depend on the strain rate, which implies that $\sigma^I = \mathbf{0}$. The stresses and internal forces can now be calculated from the above functions:

– the stress state:

$$p = \rho\,\partial_{\varepsilon_v}\psi + \rho\,\partial_{\dot{\varepsilon}_v}\Phi^* = K\left(\varepsilon_v - \varepsilon_v^p\right) - K\theta\beta_s' \qquad [13]$$

$$\mathbf{s} = \rho\,\partial_{\mathbf{e}}\psi + \rho\,\partial_{\dot{\mathbf{e}}}\Phi^* = 2G\left(\mathbf{e} - \mathbf{e}^p\right) \qquad [14]$$

$$q = 2G \left\| \mathbf{e} - \mathbf{e}^p \right\| \qquad [15]$$

with p the mean pressure $\left(= tr\frac{1}{3}\sigma \right)$, **s** the deviatoric stress tensor $\left(= \sigma - p\mathbf{I} \right)$ and q the norm of the stress deviator $\left(= \| \mathbf{s} \| \right)$.

– The consistency relationship (Eq. 9) splits into two parts:

$$\rho \partial_{\varepsilon_v^p} \psi + \rho \partial_{\dot{\varepsilon}_v^p} \Phi^* = 0 \quad \rightarrow \quad p = p_c \exp\left(- \frac{\dot{\varepsilon}_v^p}{M \left\| \dot{\mathbf{e}}^p \right\|} \right) \qquad [16]$$

$$\rho \partial_{\mathbf{e}^p} \psi + \rho \partial_{\dot{\mathbf{e}}^p} \Phi^* = 0 \quad \rightarrow \quad \mathbf{s} = - \left[\frac{\varepsilon_v^p}{\left\| \dot{\mathbf{e}}^p \right\|} + M \right] p \frac{\dot{\mathbf{e}}^p}{\left\| \dot{\mathbf{e}}^p \right\|} \qquad [17]$$

hence:

$$q = - p \left[\frac{\dot{\varepsilon}_v^p}{\left\| \dot{\mathbf{e}}^p \right\|} + M \right] \quad \rightarrow \quad M + \frac{q}{p} = \frac{- \dot{\varepsilon}_v^p}{\left\| \dot{\mathbf{e}}^p \right\|} \qquad [18]$$

This last equation represents the flow rule and corresponds to the Roscoe dilatancy rule. From these equations, it is possible to derive the expression of the loading surface:

$$q = - Mp \left(1 - \ln \frac{p}{p_c} \right) \qquad [19]$$

This relationship is equivalent to the expression of the loading surface of the Cam-clay elastoplastic model [SCH 68] and is derived, as the dilatancy rule, from the potential Φ^* (Eq. 12). To ensure that the obtained yield surface (Eq. 19) and the associated flow rule (Eq. 18) verify the thermodynamic restrictions, the potential Φ^* must be positive, convex and zero at the origin. This requirement is obtained if the following condition is verified:

$$1 + \frac{q}{Mp} = \frac{- \dot{\varepsilon}_v^p}{M \left\| \dot{\mathbf{e}}^p \right\|} < 1 \qquad [20]$$

In other words, the mean pressure must remain compressive.

[HOU 81] derived, with almost the same approach (except for the introduction of a “back stress”), the modified Cam-clay. The obtained form of the

thermodynamic potentials for the original Cam-clay (our previous results) and the modified Cam-clay are summarised and discussed in [COL 97].

The formulation of the constitutive model completes the equilibrium equation; the energy conservation equation will be fulfilled by the entropy expression:

$$s = -\partial_T \psi = -\frac{A\theta}{\rho} + \frac{\beta_s' K\left(\varepsilon_v - \varepsilon_v^p\right)}{\rho} \qquad [21]$$

from which

$$\dot{s} = -\frac{A\dot{\theta}}{\rho} + \frac{\beta_s' K\left(\dot{\varepsilon}_v - \dot{\varepsilon}_v^p\right)}{\rho} \qquad [22]$$

Then, the definition of the energy conservation equation for a thermo-elastoplastic medium is straightforward:

$$\boldsymbol{\sigma} : \dot{\boldsymbol{\varepsilon}}^p + T \cdot \left(A\dot{\theta} - \beta_s' K\left(\dot{\varepsilon}_v - \dot{\varepsilon}_v^p\right)\right) = \nabla \cdot \boldsymbol{q} \qquad [23]$$

For a small perturbation hypothesis, the specific heat under constant strain is defined as:

$$c = -\frac{AT}{\rho} \qquad [24]$$

Hence, the energy conservation equation can be written as:

$$\boldsymbol{\sigma} : \dot{\boldsymbol{\varepsilon}}^p - \rho c\dot{\theta} - \beta_s' K\left(\dot{\varepsilon}_v - \dot{\varepsilon}_v^p\right) = \nabla \cdot \boldsymbol{q} \qquad [25]$$

Hujeux model (initial version)

[HUJ 79] remarked that, where the original Cam-clay model gives satisfying results for materials with initial densities greater than the critical density (for a given confining pressure), it greatly underestimates the shear strain for overconsolidated clays. Therefore, in the initial version of his constitutive model he modified the shape of the loading surface, introducing a dependency on plastic deviatoric strain without modifying the Roscoe dilatancy rule.

Looking for a thermodynamic basis for this model, we retain the same definition for free energy as for the Cam-clay model, and the dissipation function is modified as follows:

$$\rho\Phi^* = -\frac{Mp_c \left\|\dot{\mathbf{e}}^p\right\| \left\|\mathbf{e}^p\right\|}{a + \left\|\mathbf{e}^p\right\|} \exp\left(\frac{-\dot{\varepsilon}_v^p \left(a + \left\|\mathbf{e}^p\right\|\right)}{M \left\|\dot{\mathbf{e}}^p\right\| \left\|\mathbf{e}^p\right\|}\right) \qquad [26]$$

with “a” being the positive constant parameter introduced by [HUJ 79]. The stress state will remain unchanged with respect to the previous derivation of the Cam-clay model, and the consistency relationship results in the following equations:

$$p = p_c \exp\left(\frac{-\dot{\varepsilon}_v^p \left(a + \left\| \mathbf{e}^p \right\|\right)}{M \left\| \dot{\mathbf{e}}^p \right\| \left\| \mathbf{e}^p \right\|} \right) \quad [27]$$

$$\mathbf{s} = -\left[\frac{\dot{\varepsilon}_v^p}{\left\| \dot{\mathbf{e}}^p \right\|} + \frac{M \left\| \mathbf{e}^p \right\|}{a + \left\| \mathbf{e}^p \right\|} \right] p \frac{\dot{\mathbf{e}}^p}{\left\| \dot{\mathbf{e}}^p \right\|} \quad [28]$$

Hence,

$$q = -\left[\frac{\dot{\varepsilon}_v^p}{\left\| \dot{\mathbf{e}}^p \right\|} + \frac{M \left\| \mathbf{e}^p \right\|}{a + \left\| \mathbf{e}^p \right\|} \right] p \quad [29]$$

The dilatancy rule can then be obtained from this latter relationship:

$$M \frac{\left\| \mathbf{e}^p \right\|}{\left(a + \left\| \mathbf{e}^p \right\|\right)} + \frac{q}{p} = \frac{-\dot{\varepsilon}_v^p}{\left\| \dot{\mathbf{e}}^p \right\|} \quad [30]$$

and the loading surface, as proposed by Hujeux, is obtained as:

$$q = -Mp \left(1 - \ln \frac{p}{p_c} \right) \frac{\left\| \mathbf{e}^p \right\|}{a + \left\| \mathbf{e}^p \right\|} \quad [31]$$

A discussion of the advantages of this thermodynamic derivation of constitutive models over the conventional plasticity one can be found in [HOU 82]. The reader interested by the relationship between the two functions of the thermodynamic approach (energy potential and dissipation function) and classical plasticity concepts (yield surface, plastic potential, isotropic and kinematic hardening, friction, dilation) can refer to [COL 97].

3.2. *Thermo-plastic formulation*

Conventional plasticity is now adopted to develop the thermo-mechanical formulation. In the presence of a temperature field, the analysis of plastic behaviour of soils becomes substantially more complicated due to the dependency of the yield limit on temperature. Following the elasto-plasticity principle (concept of a loading

surface f in stress space, which limits the region of elastic deformation), the total strain rate can be split into reversible and irreversible parts:

$$\dot{\varepsilon} = \dot{\varepsilon}^{Te} + \dot{\varepsilon}^{Tp} \qquad [32]$$

with $\dot{\varepsilon}^{Te}$ the reversible non-linear thermo-elastic strain rate considered as the superposition of mechanical elastic strain rate under isothermal conditions $\dot{\varepsilon}^{e}$ and the reversible thermal strain rate $\dot{\varepsilon}^{T}$:

$$\dot{\varepsilon}^{Te} = \dot{\varepsilon}^{e} + \frac{\beta_s'}{3}\dot{T}\,\delta \qquad [33]$$

where $\dot{T}$ the temperature increment and δ the Kroenecker symbol. The components of the elastic deviatoric strain obviously do not involve thermal expansions. The constitutive law is introduced as:

$$\dot{\varepsilon}^{e} = \mathbf{D}^{-1}\,\dot{\sigma} \qquad [34]$$

with ***D(T,p)*** the elastic matrix which may depend on temperature and $\dot{\sigma}$ the effective stress increment. The thermo-plastic strain rate $\dot{\varepsilon}^{Tp}$ is expressed with the normality rule as:

$$\dot{\varepsilon}^{Tp} = \lambda \cdot \partial_\sigma Q \qquad [35]$$

$\lambda(\sigma,\alpha,T) \geq 0$, is the plastic multiplier and $Q(\sigma,\alpha,T)$ the plastic potential function ($\partial_\sigma Q$ gives the direction of the plastic strain increment). α represents the internal variables modifying the yield surface $f(\sigma,\alpha,T)$. Note that, with respect to isothermal plasticity, here the loading surface also depends on temperature, i.e. a relation of the form $f(\sigma,\alpha,T)=0$ defines it. The thermo-mechanical stress increment is then given by:

$$\dot{\sigma} = D : \left(\dot{\varepsilon} - \lambda \cdot \partial_\sigma Q - \frac{\beta_s'}{3}\dot{T}\,\delta \right) \qquad [36]$$

Changes in the material state with plastic deformation are possible only if they are consistent with the yield condition, that is if (consistency equation):

$$df(\sigma,\alpha,T) = \partial_\sigma f : \dot{\sigma} + \partial_\alpha f\,\dot{\alpha} + \partial_T f \cdot \dot{T} = 0 \qquad [37]$$

Hence, it is possible to deduce the value of the plastic multiplier by introducing Eq. [36] in this last one.

4. Thermo-mechanical constitutive modelling

Under the influence of mechanical and thermal loads, saturated soils experience non-linearity and plasticity. Few models treating the numerical simulation of such elasto-thermo(visco)plastic behaviour exist in the literature. As elasto-plastic models using critical state formulations have been very successful in describing many of the more important aspects of the mechanical behaviour of soils, all existing thermo-mechanical models are based on a critical state approach. To our knowledge, [HUE 90] proposed the first constitutive thermo-mechanical law for soils explicitly including thermo-plasticity. Starting from the Cam-clay model, they introduced the thermal effect following Prager's thermo-plasticity theory. This thermal effect is incorporated at two levels: (i) reversible dilation is added to the elastic component of the strain tensor and (ii) a state variable is introduced in order to follow the evaluation of the yield surface with temperature. The obtained model treats overconsolidated (OC) conditions with thermo-elasticity, while thermo-plasticity is used for normally consolidated (NC) conditions. [ROB 96] proposed a modification of this model with the introduction of an irreversible thermal strain. More recently, a new mechanism has been added in this framework by [CUI 00]. It consists in a volumetric thermal plastic mechanism that allows for the prediction of plastic strains at high OCR values.

[LAL 93] and [MOD 92, 97] proposed cyclic elasto-thermoplastic and elasto-thermoviscoplastic constitutive models (LTVP model). This model is based on non-linear elasticity and four kinematic plastification mechanisms: one isotropic and three deviatoric. Temperature acts on the essential rheological parameters. With this structure, the LTVP model can be distinguished from other models since:

– it is one of the first cyclic thermo-viscoplastic constitutive models able to represent principal thermo-mechanical characteristics of soils over a wide range of loading (such as cyclic behaviour, even at high temperatures) and initial conditions (such as initial and induced anisotropies);

– it handles overconsolidated as well as normally consolidated clays in the same framework,

– elasto-thermoplastic formulation, when applicable, is robust and needs less model parameters but results in heavier computations,

– the isotropic thermo-plastic mechanism is able to distinguish the thermal hardening introduced by the irreversible compaction of NC clays which results in yield surface shrinkage, and the effect of the modification of the mechanical parameters which can either induce a shrinkage or a dilation of the deviatoric yield limit.

Parametric studies carried out with the help of this model show that the coupling of elasto-plastic parameters with temperature produces qualitatively different results from those of a thermo-elastoplastic model without coupling [FEL 96]. As the LTVP model seems to fit the actual knowledge on the thermo-mechanical behaviour of soils rather well, it is chosen here to illustrate the thermo-mechanical modelling of soils.

4.1. *LTVP thermo-mechanical model*

The LTVP model is a cyclic elasto-thermoviscoplastic constitutive model. It also has an alternative rate-independent version (elasto-thermoplastic). It is based on an existing isothermal orthotropic elasto-(visco)plastic multimechanism model with isotropic and kinematical hardening [AUB 85], [HUJ 85]. This model is a generalisation of the critical state theory in which the theory of coupled multimechanism elastoplasticity, as in the Koiter-Mandel theory of elastoplasticity [MAN 65], is introduced. In each plane, a plane plastic strain hypothesis is adopted. The orthotropic nature of the model stipulates that the physical co-ordinate axes be parallel to the principal stress directions. Then, the model is based on the representation of all irreversible phenomena by four coupled elementary elastoplastic mechanisms: three orthogonal deviatoric and one isotropic. These four mechanisms are activated during primary as well as during cyclic loading. Two kinds of internal parameters are needed: some subjected to a continuous flow rule and others obeying a discontinuous evolution, so that a double memory is built in the model. The second type of internal parameter is sometimes referred to as discrete-memory internal parameters, as they represent only the last loading reversal in each plane. Each deviatoric mechanism has its own hardening parameters corresponding to distortion in the corresponding plane, and all four mechanisms are coupled by the isotropic hardening parameter ε_v^p (volumetric plastic strain $= \sum_{k=1}^{4} \left(e_v^p\right)_k$). Finally, the viscoplastic implementation is obtained following [PER 63]. In the following, because of the strain history dependence, the formulation is given in the incremental form. As shown in Eq. 32, the total strain rate $\dot{\varepsilon}$ can be split into thermo-elastic and thermo-plastic parts.

Thermo-elastic component

The thermo-elastic strain rate is expressed as:

$$\dot{\varepsilon}_v^{Te} = \frac{\dot{p}}{K} + \beta_s^{'} \dot{T} \quad ; \quad \dot{\varepsilon}_d^e = \frac{\dot{\sigma}_d}{G} \qquad [38]$$

where $\dot{\varepsilon}_v^{Te}$ is the volumetric strain rate $\left(\dot{\varepsilon}_v^{Te} = tr\left(\dot{\varepsilon}^{Te}\right)\right)$ and $\dot{\varepsilon}_d^e$ the deviatoric strain rate $\left(\dot{\varepsilon}_d^e = \dot{\varepsilon}^e - \frac{1}{3}\dot{\varepsilon}_v^e I\right)$; $\dot{\sigma}_d$ is the rate of the deviatoric effective stress $\left(= \dot{\sigma}' - tr\left(\dot{\sigma}'\right) I\right)$, and $\dot{p}$ the rate of the effective mean pressure $\left(= tr\left(\sigma'\right)/3\right)$. The thermal expansion coefficient of the solid skeleton, $\beta_s^{'}$, varies strongly with temperature and slightly with pressure according to:

$$\beta_s^{'} = \left(\beta_{s0}^{'} + \zeta\, T\right)\xi \qquad [39]$$

in which $\beta_{s0}^{'}$ is the isotropic thermal expansion coefficient at reference temperature T_0, and ξ the ratio between the critical state pressure for the initial state p_{c0} and the mean effective pressure p at ambient temperature:

$$\xi = \frac{p_{c0}}{p} \qquad [40]$$

ς corresponds to the slope of the variation of $\beta_s^{'}$ with respect to current temperature T at $\xi = 1$. This formulation enables the thermo-elastic strain rate to increase with overconsolidation ratio and temperature. The elastic moduli are given by :

$$K = K_{ref}\left(\frac{p}{p_{ref}}\right)^n \qquad G = G_{ref}\left(\frac{p}{p_{ref}}\right)^n \qquad [41]$$

where K_{ref} and G_{ref} are the bulk and shear elastic moduli, respectively, at a reference pressure p_{ref} (the value of mean effective pressure at which the elastic moduli are measured), and n is the non-linear elasticity exponent. Due to the lack of any significant information on the dependency of elastic moduli on the temperature of soils, here we have assumed that *K* and *G* are independent of temperature and vary only with the mean effective pressure. Meanwhile, the material may exhibit thermo-plastic behaviour due to a change of temperature which induces a change in the mean effective pressure. In this case, we have a variation of *K* and *G* induced by the variation of the mean effective pressure caused by the temperature change.

At this point, it should be recalled that the generally accepted hypothesis that thermal elastic strain is isotropic has been assumed. However, it could also be possible to assume isotropic thermal stress.

Thermo-viscoplastic strain rate component

The irreversible thermal effects are introduced by taking into account the dependence of yield surface, flow rule and internal variables on temperature. The monotonous loading conditions are designated by the letter "*m*" and the cyclic loading conditions by "*c*".

Deviatoric mechanisms

In order to take into account the anisotropy induced by the stress path, three deviatoric yield surfaces are written in three orthogonal planes (mechanisms $k; k = \{1,2,3\}$) of the stress space (Fig. 9). In each plane, a plane plastic strain hypothesis is assumed and a limit criterion very close to that of Mohr-Coulomb is obtained, and its yield function is that of Cam-clay. Then, the deviatoric monotonous yield surface for mechanism *k* is proposed as:

$$f_k^m = q_k - p_k \, F_k \, r_k^m \sin\phi \qquad [42]$$

where p_k and q_k are the *reduced mean effective pressure* and *deviatoric stress*, respectively, in the plane of each deviatoric mechanism *k* (see Fig. 10), given as:

$$q_k = \|\mathbf{s_k}\| = \frac{1}{2}\left[\left(\sigma'_{ii} - \sigma'_{jj}\right)^2 + 4\,\sigma'^2_{ij}\right]^{1/2} \qquad k = \{3,2,1\};\ i,\ j = \{1,2\},\{1,3\},\{2,3\} \qquad [43]$$

$$p_k = \frac{\left(\sigma'_{ii} + \sigma'_{jj}\right)}{2}$$

with the vector $\mathbf{s}_k = \left(\frac{1}{2}\left(\sigma'_{ii} - \sigma'_{jj}\right)\sigma'_{ij}\right)_k$. We note that σ'_{ij} is a component of the tensor σ (indicial notation is not used here). The function F_k takes into account the volumetric hardening or softening with respect to the critical state as:

$$F_k = 1 - b\left(L_n \frac{P_k}{p_{c0}} - \beta\, \varepsilon_v^{T_p}\right) \qquad [44]$$

with *b* a parameter that controls the shape of the yield surface (b=0 Mohr-Coulomb; b=1 Cam-clay). The internal variable r_k^m represents the ratio of the mobilised friction over the maximum friction that may be mobilised. It permits the decomposition of the behaviour domain into elastic, hysteretic and mobilised domains introduced by other model parameters termed r_{el}, r_{hys} and r_{mob}. It is possible to normalise the monotonous yield surface as:

$$\mathfrak{I}_k^m = \frac{\|\mathbf{s}_k\|}{p_k \; f_k \sin\phi} - r_k^m \qquad [46]$$

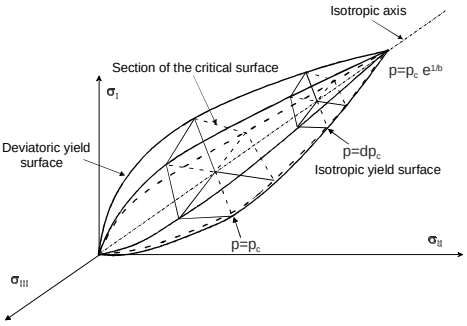

Figure 9. *Yield surfaces in principal stress plane*

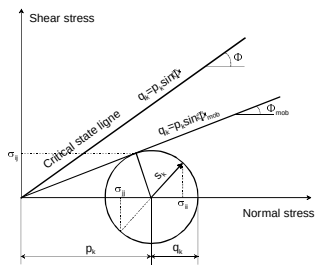

Figure 10. *Stress state in the (i, j) plane of the deviatoric mechanism k*

Hence, the normalised monotonous yield surface in the plane of the mechanism k is a circle with radius r_k^m, evolving during loading. Variables F_k and r_k both introduce isotropic hardening but have different evolution rules and different origins, as well. The first one introduces the isotropic hardening associated with the plastic volumetric strain as in the Cam-clay model. The second one represents the isotropic hardening caused by the deviatoric plastic strain in each mechanism. The mechanisms are coupled only due to the first one, as the second is attached to each physical plane representing the deviatoric mechanism. ϕ is the friction angle at the critical state varying with temperature as:

$$\phi = <\phi_0 - g\,T> \qquad [47]$$

where ϕ_0 is the value of the friction angle at the ambient temperature and g is an average slope of variation of the friction angle with temperature, which can be either positive or negative. The symbol <.> designates the Macauly brackets: [<x> = x if x ≥ 0; <x> = 0 otherwise]. Obviously, the values of g and ϕ_0 obtained from experiments always result in positive values for the friction angle in the considered range of temperature. The yield surface is extended for the cyclic loading using discrete-history internal parameters.

Thermoplasticity/Thermoviscoplasticity

The yield surface presented in the last section may be included in the framework of elastoplasticity or viscoplasticity. The plastic flow rule is derived for each mechanism k, and the plastic strain rate becomes:

$$\begin{aligned} \left(\dot{e}_v^{Tp}\right)_k &= \left(\dot{\varepsilon}_{ii}^{Tp} + \dot{\varepsilon}_{jj}^{Tp}\right)_k = \dot{\lambda}\cdot\left(\Psi_v\right)_k \\ \left(\dot{\mathbf{e}}_d^{Tp}\right)_k &= \left(\left(\dot{\varepsilon}_{ii}^{Tp} - \dot{\varepsilon}_{jj}^{Tp}\right)\dot{\varepsilon}_{ij}^{Tp}\right)_k = \dot{\lambda}\cdot\left(\boldsymbol{\Psi}_d\right)_k \end{aligned} \qquad k=\{3,2,1\},\ i,\ j=\{1,2\},\{1,3\},\{2,3\} \qquad [48]$$

The direction of plastic flow in each mechanism is obtained by assuming the normality rule in the deviatoric plane together with a modified Roscoe's dilatancy rule. $\left(\Psi_v\right)_k$ and $\left(\boldsymbol{\Psi}_d\right)_k$ are thus defined by:

$$\begin{aligned} \left(\Psi_v\right)_k &= -\alpha_k^{\Xi}\left(\sin\varpi - \frac{\left[\mathbf{s}_k\cdot\left(\boldsymbol{\Psi}_d\right)_k\right]}{p_k}\right) \\ \left(\boldsymbol{\Psi}_d\right)_k &= \partial_{\mathbf{s_k}} f_k^{\Xi} \end{aligned} \qquad \Xi = m \text{ or } c \qquad [49]$$

where ϖ is the dilatancy angle corresponding to the characteristic line. The plastic multiplier $\dot{\lambda}$ is evaluated from the persistency (or consistency) condition, i.e. $\dot{\lambda}\dot{f} = 0$. One can refer to [HUJ 85] for additional information on the parameter α_k^{Ξ}, which may vary with r_k^{Ξ} and adjusts the dilatancy during shearing.

The rate-dependent LTVP version (thermo-viscoplastic) is a Perzyna-type viscoplastic model. Thus, the following relationships may be used for evaluating the irreversible strain for each mechanism k:

$$\left(\dot{e}_v^{Tvp}\right)_k = \frac{\left\langle \frac{f_k^{\Xi}}{f_0} \right\rangle^{n_\mu}}{\mu} \cdot \left(\Psi_\upsilon\right)_k \qquad \Xi = m \text{ or } c \qquad [50]$$

$$\left(\dot{\mathbf{e}}_d^{Tp}\right)_k = \frac{\left\langle \frac{f_k^{\Xi}}{f_0} \right\rangle^{n_\mu}}{\mu} \cdot \left(\boldsymbol{\Psi}_d\right)_k$$

where μ is a measure of viscosity which may vary with temperature. It may be concluded that as μ tends to zero, the rate-independent (thermoplastic) version is recovered. f_0 is a reference stress introduced for dimensional requirements (here taken equal to 1 MPa). The direction of plastic flow in each mechanism is the same as in Eq. 49. The following viscosity law may be adopted by analogy with the temperature-dependence of water's viscosity:

$$\mu = \eta e^{\zeta/T} \qquad [51]$$

where η and ζ are physical constants. n_μ is a material viscosity parameter. The choice of the viscosity law identical to that of water may be made during the first approximation as a plausible hypothesis in the absence of data concerning such a law for the materials studied. In general, to obtain the model parameters (remembering that elastoplasticity is an asymptotic state for such a viscoplastic model), the best strategy is to perform tests with a very low loading rate in order to determine the “elastoplastic”-type parameters (rate-independent) first, and then with higher loading rates for viscosity-type parameters. These latter may be replaced by creep-type tests. The viscosity exponent n_μ may be determined using creep tests with several loading steps. In all of the numerical applications presented in this paper, n_μ has been assumed equal to unity and μ has been supposed to be constant. Without specific tests, it is not possible to determine these quantities.

The evolution rule for the degree of mobilised friction is given by the following relationship:

$$\dot{r}_k^m = \frac{\left(1 - r_k^m\right)^2}{a} \frac{\left\langle \frac{f_k^m}{f_0} \right\rangle^{n_\mu}}{\mu} \quad \text{and} \quad \dot{r}_k^c = \frac{\left(1 - r_k^c\right)^2}{a} \frac{\left\langle \frac{f_k^c}{f_0} \right\rangle^{n_\mu}}{\mu} \frac{\left\| \mathbf{s}_k^c \right\|}{\left\| \mathbf{s}_k^c \right\| - \mathbf{n}_k \cdot \mathbf{s}_k^c} \qquad [52]$$

Isotropic mechanism

With only deviatoric mechanisms, no irrecoverable strain is developed under isotropic loading conditions. Thus, an isotropic mechanism is necessary for taking such effects into account. For thermal loading conditions, this mechanism plays a very crucial role. The isotropic yield surface is proposed as:

$$f_{iso}^{\Xi} = \left|\pi^{\Xi}\right| - dp_{c0}\, e^{\beta\varepsilon_v^{Tp}}\, r_{iso}^{\Xi} \quad \Xi = m \text{ or } c \qquad [53]$$

where $\pi^m = p, \pi^c = p - \left(D_{iso} - n_{iso} r_{iso}^c\right) dp_{c0}\, e^{\beta\varepsilon_v^{Tp}} \cdot r_{iso}^{\Xi}$ is the ratio of the isotropic mechanism. It evolves from a minimum, which defines the elastic domain to unity at the perfectly plastic state. Its evolution is controlled by variation of total plastic volumetric strain. D_{iso} is the normalised mean effective pressure at the unloading (or reloading) point, and n_{iso} (= -1 or +1) indicates the direction of the previous loading [AUB 85], [HUJ 85]. In the "$e - Ln(p)$" plane, d represents the distance between the critical state line at ambient temperature and the isotropic consolidation curve for a given temperature (Fig. 11). As the isotropic consolidation line moves toward the perfect plasticity (critical state) line with increasing temperature, the following relationship is assumed for modelling this phenomenon:

$$d = d_0 \exp(-\beta\, \chi) \qquad [54]$$

χ *(T)* is the variation of void ratio with temperature modelled by:

$$\chi = \frac{T - T_0}{a_t (T - T_0) + b_t} \qquad [55]$$

a_t and b_t being numerical parameters determined from experimental results. d_0 is the value of parameter d at $T = T_0$. The expression for d implicitly assumes that the volume variation due to thermal expansion (reversible part) is negligible compared to that caused by thermoplasticity. This assumption may be verified using usual values for thermal expansion coefficients and observed settlement in heated samples. Moreover, the variation of thermally-induced volumetric plastic strain follows a hyperbolic evolution with temperature increase for normally consolidated clays. The plastic strain rate may be calculated as:

$$\left(\dot{\varepsilon}_v^{Tp}\right)_{so} = \dot{\lambda}\left(\Psi_v\right)_{iso} \qquad [56]$$

for the thermoplastic formulation, and by:

$$\left(\dot{e}_v^{Tvp}\right)_{so} = \frac{\left\langle \frac{f_{iso}^{\Xi}}{f_0} \right\rangle^{n_\mu}}{\mu} \left(\Psi_v\right)_{iso} \quad \Xi = m \text{ or } c \qquad [57]$$

for the rate-dependent constitutive version.

In both formulations, an associated flow rule is assumed. The thermo-viscoplastic strain increment is thus proportional to:

$$\left(\Psi_v\right)_{iso} = \frac{1}{3} sgn\left(\pi^{\Xi}\right) \quad \Xi = m \text{ or } c \qquad [58]$$

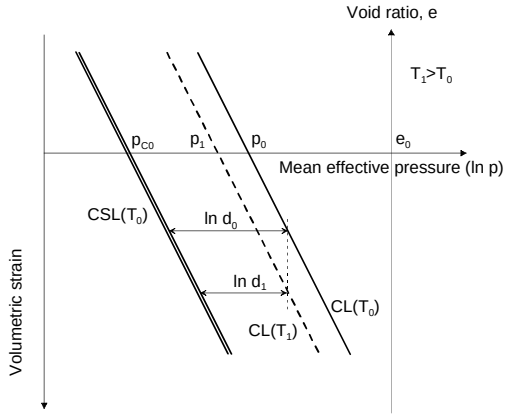

Figure 11. *Definition of the parameter d*

4.2. *Sensitivity of yield surface to temperature*

Sensitivity of yield surface to temperature is related to the evolution of the representative stress point due to thermal loading. Classical plasticity is used and once the yield limit has been reached, so that $f_k = 0$, an irreversible strain takes place in the material in addition to the reversible one. The hypothesis of continuous contact of the yield surface with the constant effective stress point during heating is adopted. This hypothesis has been experimentally confirmed by [BAL 85].

Isotropic yield surface
The isotropic yield surface is assumed to follow the evolution presented in Fig. 12:

– In a normally consolidated state: the initial state is given by the point (0) in which the stress representative point p_0 is located on the yield loading f_0 so that an increase in temperature ($\Delta T = T_1 - T_0$) yields a decrease in the distance d (Eq. 54), resulting in a shrinkage of the isotropic yield surface (1). With an elastoplastic assumption and to sustain constant effective stress during heating, an instantaneous volumetric plastic strain is generated (isotropic hardening) in order to maintain the yield surface f_1 on the stress point. In a viscoplastic formulation, the yield surface will gradually regain the stress point with the generation of the volumetric plastic strain modulated by the viscosity of the materials.

– In an overconsolidated initial state (Fig. 12-overconsolidated state), the stress point p_0 is initially inside the yield surface f_0 due to the high value of the critical state pressure p_c with respect to the initial state p_{c0}. During heating and under drained conditions and an isotropic stress state, a dilational thermoelastic strain is generated (Eq. 38). Moreover, d decreases according to Eq (54), resulting in shrinkage of the isotropic yield surface (1). If the shrinkage is insufficient, the thermal strain obtained is reversible. Otherwise, the yield limit will reach the stress point and then the model will behave as in the case of a normally consolidated state by regenerating thermoplastic compaction.

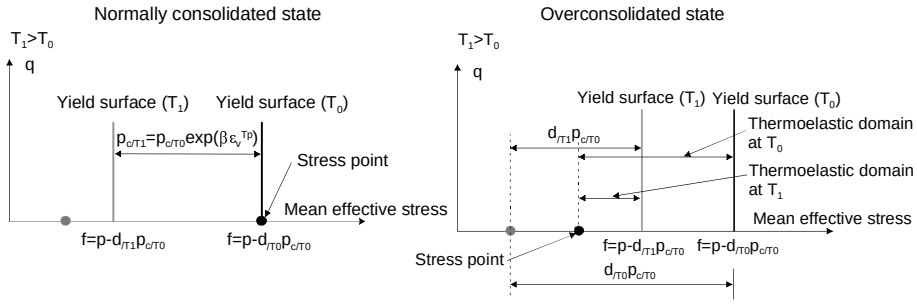

Figure 12. *Evolution of the normalised isotropic yield surface with temperature*

Deviatoric yield surface

The coupling between deviatoric and isotropic mechanisms by the volumetric hardening parameter (volumetric plastic strain) results in an expansion of deviatoric yield surfaces during thermal loading. On the other hand, there may be a decrease in the value of the friction angle (Eq. 47), which may counterbalance the first effect. In an elastoplastic formulation, the stress point must remain constantly on the yield surface, thus instantaneous deviatoric plastic strain is generated. During cooling, the deviatoric yield surfaces expand due to the increase of friction angle and the material behaves almost like a thermoelastic material with reversible strain. A particular case could exist in which the previous two opposite phenomena produce

no variation in the stress point and thus no plastic deformation. Such a case is called a neutral change of state [PRA 58].

Finally, in the thermo-viscoplastic formulation, the variation of the viscosity with temperature may largely affect the amplitude of thermally induced strain.

4.3. *Thermomechanical behaviour under undrained conditions*

Under undrained conditions, thermal and mechanical loading generate pore pressure variations. According to [CAM 68], a temperature change of 1°C may produce an excess pore pressure of about 1.5% of the mean effective pressure. Assuming that the water is linearly compressible, the pore pressure variation is given by [LAL 93]:

$$n\beta'_f \dot{p}_f = -\dot{\varepsilon}_v + \left[n\beta'_f + (1-n)\left(\beta'_{so} + \varsigma T\right)\xi\right]\dot{T} \qquad [59]$$

where n is the effective porosity of the solid skeleton relative to the volume occupied by the free water only, and p_f and β'_f are the pore pressure and the compressibility of free water, respectively. Therefore, the variation of the free-water pore pressure is attributed to two factors: the variation of the skeletal volume (compaction or dilation) and the thermal dilation of the free water. The thermal expansion coefficient of water depends on temperature and, in some way, on pressure.

5. Numerical simulations

Numerical validations and analyses of the capacity of the LTVP constitutive model to predict the major thermo-mechanical aspects of the behaviour of soils can be found in [LAL 93], [MOD 97], [LAL 01]. Performances of this model are illustrated here with the simulation of the behaviour of three different materials.

5.1. *Numerical modelling of the behaviour of Boom Clay*

The mechanical parameters have been identified using two undrained triaxial tests [HOR 85] at two confining pressures (2.85 MPa and 5.42 MPa, Fig. 13), and an isotropic consolidation test at ambient temperature [BAL 91]. The thermal parameters were determined using a thermal loading path, which was already presented in Section 2 (Fig. 3). The NC initial state and the overconsolidated one were used with the assumption that in the OC state the behaviour is thermo-elastic. Therefore, only the slightly overconsolidated case (OCR=2) corresponds to a

numerical prediction. Comparison between numerical prediction and experimental results is satisfactory during thermal loading and unloading (Fig. 14).

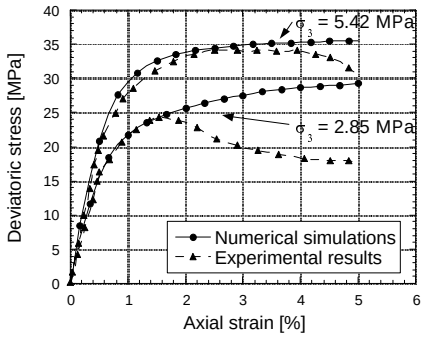

Figure 13. *Boom clay: back-prediction modelling compared with experimental results –undrained triaxial tests [HOR 85]*

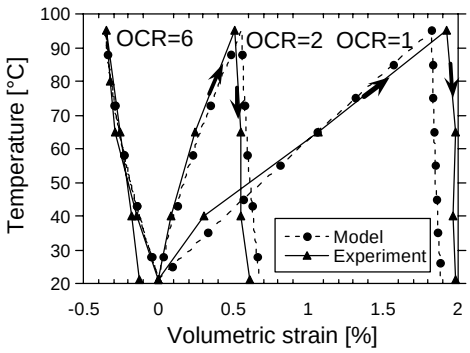

Figure 14. *Boom clay: Numerical modelling of a thermal cycle [BAL 91]*

	Boom Clay	Pontida Clay	MC Clay
Elastic [*Kref, Gref, n*] [MPa][MPa][-]	150, 130, 0.4	200, 150, 0.6	80, 37, 0.5
Plastic [ϕ_0, β, p_{c0}] [°][-][MPa]	19.5, 14, 6	35, 51.5, 1.1	18, 11, 0.1
Dilatancy [ψ] [°]	23	24.5	18
Hardening [b, d_0] [-] [-]	0.6, 1.3	0.3, 1.2	0.9, 2.1
Domains [r_{el}, r_{hys}, r_{mob}] [-] [-] [-]	1E-3 , 0.01, 0.1	1E-4, 1E-3, 0.01	1E-3, 0.2, 0.9
Thermal [β'_s, g, a_t, b_t] [C^{-1}] [-] [-] [-]	1.3E-5, 8.5E-3, 0.5, 3350	1.3E-5, 6E-3, 0.16, 1	3E-5, 35E-5, 37, 2222

Table 1. *LTVP model parameters' for Boom clay, Pontida clay and MC clay*

Using the parameters obtained, a coupled thermo-mechanical (isotropic) path was simulated (Fig. 15). It should be noted here that the first part of the loading path (isotropic consolidation from 1.5 to 3 MPa and first thermal loading from 22 to 88°C) was used for calibrating the model parameters. The predictions are quite satisfactory in the volumetric strain/temperature plane. The only difference occurs during thermal unloading in the overconsolidated state, where the model predicts a dilation as opposed to the experimental behaviour. In the volumetric-strain/mean-

pressure plane, the experimental results show that the apparent volumetric stiffness is independent of temperature. This is not the case in the model conception.

However, in general, the numerical predictions in this isotropic case remain quantitatively acceptable.

5.2. *Numerical modelling of the behaviour of Pontida Clay*

Numerical simulations of triaxial shear tests conducted on remoulded Pontida Clay are presented in this section. These tests were carried out at two different temperatures for two different overconsolidation ratios (OCR = 5 and 12.5) [BAL 91]. The model parameters (Table 1) were determined using the triaxial tests at ambient temperature (back-prediction in Fig. 16). Numerical simulations tests at 95°C are presented in Fig. 17 and show that the model is able to take into account the decrease of the dilatancy (for OCR=5) and the strength (for OCR=12.5) induced by heating.

In Fig. 18, numerical predictions compared with experimental results of an undrained creep and heating test on an initially anisotropic sample are presented. The experimental path [HUE 91] consists of imposing a deviatoric stress of 1.2 MPa on an initially consolidated sample at 2.5 MPa.

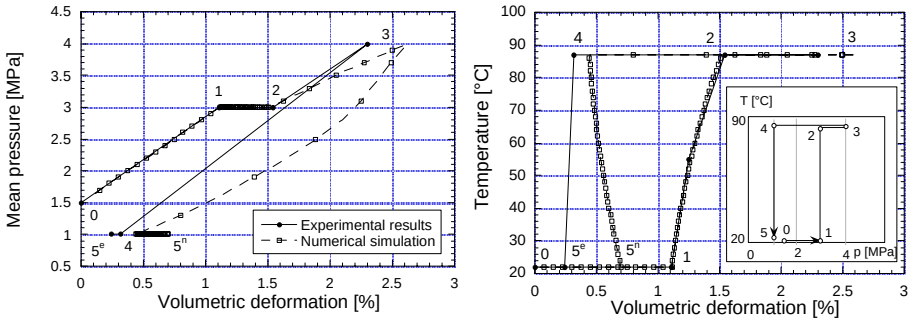

Figure 15. *Boom clay: numerical modelling of a coupled thermo-mechanical path*

After 48 hours, during which the sample creeps, a thermal loading is applied at 1°C per hour. In the main effective-deviatoric stress plane, the correspondence between prediction and experiment is good. In the axial strain/excess pore pressure plane, the prediction is less satisfactory. This is due to the prediction of the induced strains by the deviatoric stress, which is 50% less than that measured. This difference is present in the next creep and heating steps. However, the model predicts an increase in pore pressure, which brings about the decrease of the main effective stress and the failure of the sample.

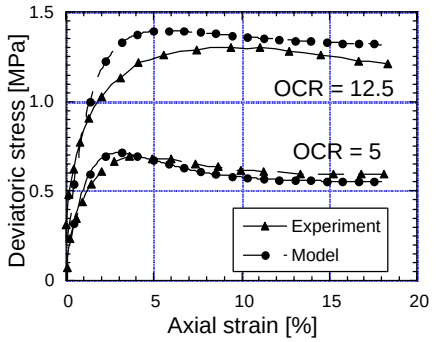

Figure 16. *Pontida clay: back-prediction modelling compared with experimental results for two drained triaxial tests at 20°C [BAL 91]*

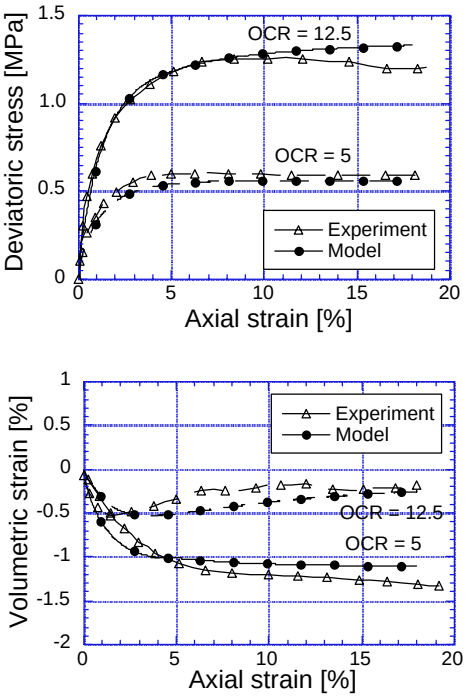

Figure 17. *Pontida clay: back-prediction modelling compared with experimental results for two drained triaxial tests at 95°C [BAL 91]*

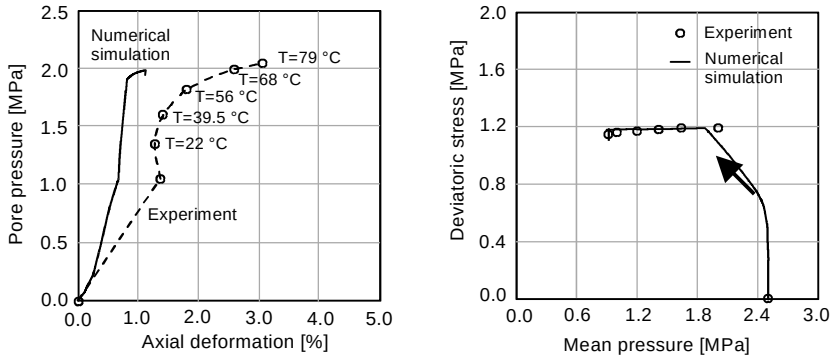

Figure 18. *Pontida clay: numerical prediction of thermal failure under undrained conditions [HUE 91]*

5.3. *Numerical modelling of the behaviour of MC Clay (kaolin)*

Experimental results on reconstituted samples from clay slurry made by mixing MC (Kaolin) clay and water [KUN 91, 95] were simulated. The presented experimental results were obtained for the paths in Fig. 19 (Path 1: conventional undrained triaxial test at room temperature; consolidation from 20 to 196 kPa at 20°C followed by shearing under undrained conditions; Path 2 ($0\rightarrow1\rightarrow2$): Identical consolidation as for Path 1, followed by heating up to 90°C under drained conditions before shearing; Path 3 ($0\rightarrow3\rightarrow4\rightarrow2$): consolidation from 20 to 137kPa; heating up to 90°C under drained conditions; consolidation pressure increasing up to 196 kPa then shearing; Path 4 ($0\rightarrow1\rightarrow2\rightarrow1$): consolidation up to 196kPa; heating up to 90°C; cooling under drained conditions; shearing under undrained conditions. Another path was followed but is not shown in the figure (Path 5): thermal loading in oedometer conditions. Experimental tests for Paths 1 to 4 were carried out twice.

Calibration of model parameters and back-predictions

The material parameters of the MC clay for the LTVP constitutive model were determined using four tests: two triaxial shear tests in NC and OC states at room temperature (20°C, Path 1 for NC), one triaxial test at high temperature (90°C, Path 2) and one thermal loading (Path 5). Fig. 20 shows the identification of the thermal parameters a_t and b_t (Eq. 55). Back-predictions of the experimental results are shown in Fig. 21 (triaxial shear tests in NC and OC states at room temperature, 20°C) and in Fig. 22 (triaxial shear tests in NC state at room and high temperatures (Paths 1 and 2)). One can easily notice the good quality of the back-prediction, except for the pore water generation at small strains.

Numerical prediction of thermo-mechanical loading tests

Numerical predictions and experimental results on Paths 2 and 3 are given in Fig. 23. The goal here is to identify the influence of the path followed on the undrained mechanical behaviour of the clay at high temperature (90 °C). In Path 2, consolidation brings about mechanical hardening, then the increase in temperature produces thermal hardening. In Path 3, the mechanical hardening is produced until 137kPa at ambient temperature, then the thermal hardening is activated by heating up to 90°C. This thermo-plastic hardening increases the mechanical yield surface without any change in the stress tensor. For this condition, the yield point is inside the yield surface and the next consolidation imposed is initially elastic (until the yield point reaches the yield limit), then elasto-plastic. No differences can be found in shear strength for both cases, indicating the negligible influence of the thermal state on mechanical hardening. Numerical predictions compare well with experimental results.

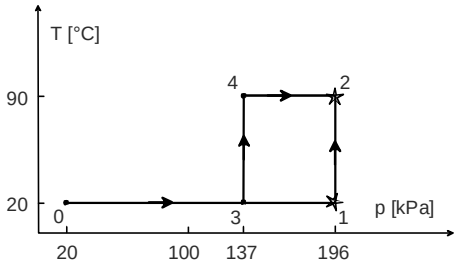

Figure 19. *MC clay: experimental paths: stars mark points at which samples are sheared*

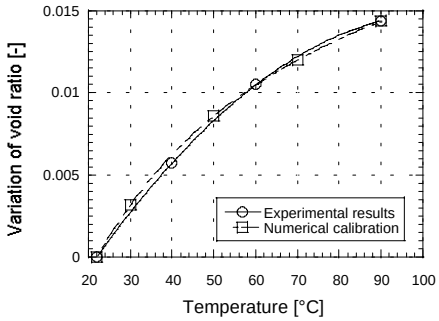

Figure 20. *MC clay: variation of void ratio versus temperature [KUN 91]*

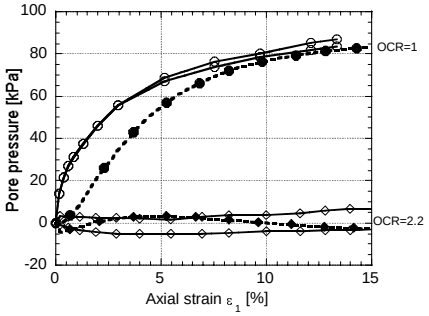

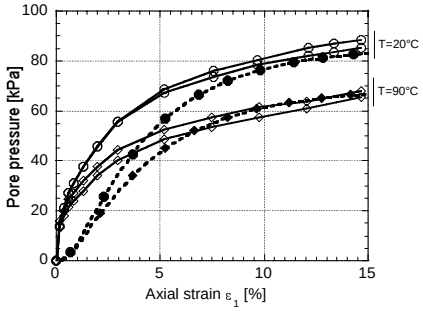

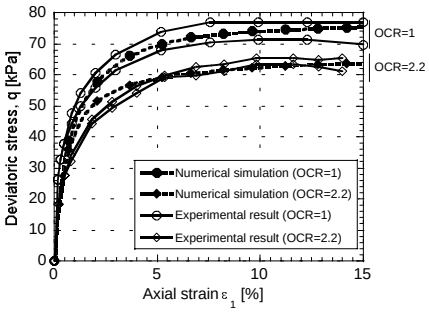

Figure 21. *MC clay: numerical back-prediction and experimental results for undrained shear tests at room temperature in NC and OC states [KUN 91]*

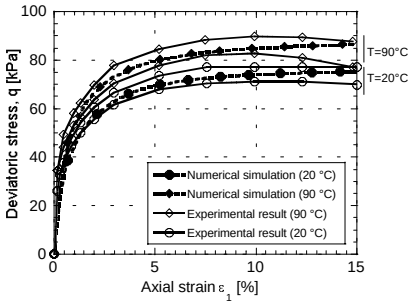

Figure 22. *MC clay: numerical back-prediction and experimental results for undrained shear tests at different temperatures (paths 1 & 2) [KUN 91]*

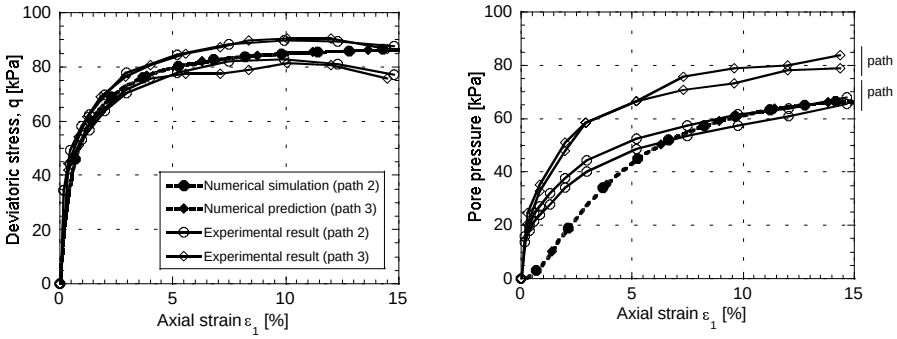

Figure 23. *MC clay: numerical predictions and experimental results for undrained shear tests (Paths 2 & 3) [KUN 91]*

Cyclic behaviour

Heating has an important influence on the cyclic stress-strain behaviour of soils. To show the modelling capacity of such phenomena, some numerical predictions are presented here. The simulated experiments were carried out by [KUN 91]. Two specimens were consolidated at a pressure of 196 kPa at room temperature. Then, one of them was cyclically sheared in undrained conditions at room temperature while the other was heated up to 90 °C in drained conditions and after that was cyclically sheared in undrained conditions at this temperature. The same deviator stress of 65 KPa was applied in both cases. The comparison between the behaviours of the heated and the unheated samples shows that the strain induced by the cyclic shearing is smaller in the heated case and that the induced pore pressure is significantly smaller for the heated sample. These results support the previous statement that heating induces thermal hardening. A larger increase in pore pressure for the unheated sample results in smaller values of mean effective pressure than for the heated one. Numerical predictions clearly show the capacities of the LTVP model for mechanical cyclic paths at different temperatures.

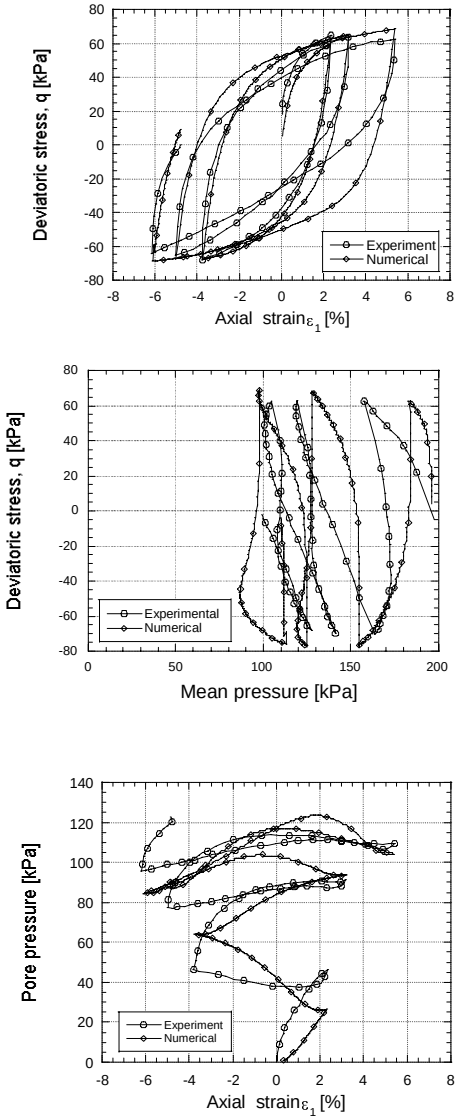

Figure 24. *MC clay: numerical predictions and experimental results for cyclic undrained shear tests at 20 °C [KUN 91]*

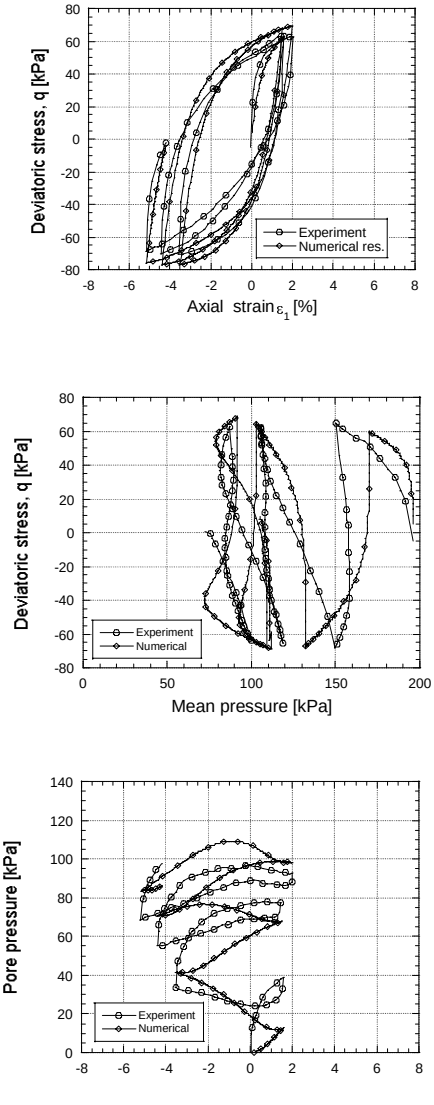

Figure 25. *MC clay: numerical predictions and experimental results for cyclic undrained shear tests at 90°C [KUN 91]*

6. Conclusions

As the range of potential problems in geomechanics with non-isothermal conditions becomes increasingly wider, it is important to understand and to improve the modelling of such behaviour. This paper addressed the state of developments in three topics related to this subject: experimental evidence, theoretical framework and constitutive modelling. An introduction to thermodynamics of irreversible processes with internal variables is also given to show that it offers an appropriate framework to introduce constitutive equations.

Acknowledgements

The author wish to express his thanks to L. Vulliet for his encouragement and C. Cekerevac for his help in the preparation of this paper. This paper is a compilation of several works from which large portions were obtained while the author was at the BRGM and Ecole Centrale Paris and published with H. Modaressi and D. Aubry. He thanks them for their collaboration.

Appendix 1: Thermo-mechanical behaviour of unsaturated soils

Information available on the thermo-mechanical behaviour of unsaturated soil is very limited and not sufficient to permit the development and validation of comprehensive constitutive laws. In spite of this, interesting frameworks for the modelling of the thermo-mechanical behaviour of unsaturated soils are proposed, even in absence of calibration data. [GEN 95] presented a constitutive model based on a generalisation of the Cam-clay yield surface in stress, suction and temperature space. A prospective version of the LTVP model exists for unsaturated soils [MOD 95]. In this version, the influence of suction variation on the void ratio is added to those of temperature which modify the critical pressure in this way. Some of the very few available experimental results are used in an attempt to validate this model.

7. References

[AUB 85] AUBRY D., KODAISSI E. & MEMOIN Y., "A viscoplastic constitutive model for clays including a damage law", *Proc. of 5th International Conference on Numerical Methods in Geomechanics*, Nagoya, p. 421-428, 1985.

[BAL 91] BALDI G., HUECKEL T., PEANO A. & PELLEGRINI R., Developments in modelling of thermo-hydro-geomechanical behaviour of Boom clay and clay-based buffer materials, Report EUR 13365, Commission of the European Communities, Nuclear science and technology, 1991.

[BAL 85] BALDI G., BORSETTO M., HUECKEL T. & TASSSONI E., "Thermally induced strains and pore pressures in clays", *International symposium on environmental geotechnology*, Allentown, p. 391-402, 1985.

[BIO 56] BIOT I.M.A., "Thermoelasticity and irreversible thermodynamics", *J. Appt. Phys*., 27, p. 240-253, 1956.

[BOU 94] BOUDALI M., LEROUEIL S. & SRINIVASA MURTHY B.R., "Viscous behaviour of natural clays", *Proceedings of 13th ICSMFE*, New Delhi, 1:411-416, 1994.

[BUR 85] BURGER A., RECORDON E., BOVET D., COTTON L. & SAUGY B., *Thermique des nappes souterraines*, Presses polytechniques romandes, 1985.

[CAM 69] CAMPANELLA R.G. & MITCHELL J.K., "Influence of temperature variations on soil behaviour", *Journal of Soil Mechanics and Foundations division*, ASCE, 94, p. 709-734, 1968.

[CEK] CEKEREVAC C., Thermo-hydro-mechanical behaviour of saturated soils – application to thermal piles, PhD thesis, Swiss federal Institute of Technology, Lausanne – In preparation.

[COL 97] COLLINS I.F. & HOULSBY G.T., "Application of thermomechanical principles to the modelling of geotechnical materials", *Proc. Royal society of London*, 453, 1975-2001, 1997.

[CUI 00] CUI YJ, SULTAN N. & DELAGE P., "A thermomechanical model for saturated clays", *Can. Geotech. Journal*, 37 (3): 607-620, 2000

[DEM 82] DEMARS K.R. & CHARLES R.D., "Soil volume changes induced by temperature cycling", *Can. Geotech. Journal*, vol. 19, p. 188-194, 1982.

[DES 76] DESPAX D., Influence de la température sur les propriétés mécaniques des argiles saturées, Doctoral thesis, Ecole Centrale Paris, 1976.

[DUS 88] DUSSEAULT M.B., WANG Y. & SIMMONS J.V., "Induced stresses near a fire flood front", *AOSTRa J. Res*, 4, p. 153-170, 1988.

[ERI 89] ERIKSON L.G., "Temperature effects on consolidation properties of sulphide clays", *Proceedings of the 12th International Conference on Soil Mechanics and Foundation Engineering*, 3, 2087-2090, 1989.

[FEL 96] FÉLIX B., LEBON P., MIGUREZ R. & PLAS F., "A review of the ANDRA's research programmes on the thermo-hydromechanical behaviour of clay in connection with the radioactive waste disposal project in deep geological formations", *Engineering Geology*, 41:35-50, 1996.

[FLE 79] FLEUREAU J.M., Influence d'un champ thermique ou électrique sur les phénomènes d'interaction solide-liquide dans les milieux poreux, Doctoral thesis, Ecole Centrale de Paris, 1979.

[GEN 95] GENS A., "Constitutive laws", in *Modern issues in non-saturated soils*, eds. Gens A., Jouanna P. & Schrefler B.A., p. 129-158, Springer-Verlag, 1995.

[GER 83] GERMAIN P., NGUYEN Q.S. & SUQUET S., "Continuum thermodynamics", *J. Appt. Mech. ASME*, 50,1010-1020, 1983.

[HAL 75] HALPHEN B. & NGUYEN Q.S., "Sur les Matériaux Standard Généralisés", *J. de Mécanique*, vol. 14, n° 1, 39-63, 1975.

[HOR 85] HORSEMAN S.T., WINTER M.G. & ENTWISTLE D.C., "Geotechnical characterisation of Boom clay in relation to the disposal of radioactive waste", *Natural Environment Research Council*, Report FLPU 86-12, British Geological Survey, 1985.

[HOU 81] HOULSBY G.T., A study of plasticity theories and their applicability to soils, Ph.D Thesis, University of Cambridge, 1981.

[HOU 82] HOULSBY G.T., "A derivation of the small-strain incremental theory of plasticity from thermomechanics", *IUTAM Conference on Deformation and Failure of Granular Materiats*, p. 109-118, 1982.

[HUE 89] HUECKEL T. & PELLEGRINI R., "Modeling of thermal failure of saturated clays", in *Numerical models in geomechanics*, 81-90, Elsevier, 1989.

[HUE 89] HUECKEL T. & PELLEGRINI R., "Thermo-plastic modeling of undrained failure of saturated clay due to heating", *Soils and Foundations*, 31:1-16, 1991.

[HUE 90] HUECKEL T. & BORSETTO M., "Thermoplasticity of saturated soils and shales: Constitutive equations", *Journal of Geotechnical Engineering*, 116:1765-1777, 1990.

[HUJ 79] HUJEUX J.-C., Calcul numérique de problèmes de consolidation elastoplastique, Doctor of Engineering Thesis, Ecole Centrale de Paris, 1979.

[HUJ 85] HUJEUX J.-C., "Une loi de comportement pour le chargement cyclique des sols", in V. Davidovici ed., *Genie Prasismique*, Presses de l'ENPC, p. 287-353, 1985.

[KUN 91] Kuntiwattanakul P., "Effect of High Temperature on Mechanical Behaviour of Clays". Doctoral thesis, University of Tokyo, 1991.

[KUN 95] KUNTIWATTANAKUL P., TOWHATA I., OHISHI K., & SEKO I., "Temperature effects on undrained shear characteristics of clay", *Soils and Foundation*, 35(1), p. 147-162, 1995.

[LAL 93] LALOUI L., Modélisation du comportement thermo-hydro-mecanique des milieux poreux anélastique, Doctoral thesis, Ecole Centrale Paris, 1993.

[LAL 94] LALOUI L. & MODARESSI H., "Effets de la Thermo-Plasticite des argiles sur le comportement des puits de stockage", *1st International Congress on Environmental Geotechnics*, Edmonton, p. 881-887, Ed. BiTech publishers Ltd. 1994.

[LAL 99] LALOUI L., MORENI M., FROMETIN A., PAHUD D. & VULLIET L., "In-Situ Thermo-Mechanical Load Tests on a Heat Exchanger Pile", *Proceedings of 4th Intenational Conference on Deep Foundation Practice incorporating Piletalk*, Singapore, p. 273-279, 1999.

[LAL 01] LALOUI L., CEKEREVAC C. & VULLIET L., "Thermo-mechanical modelling of the behaviour of MC clay", *Proceedings of the 10th International Conference on Computer Methods and Advances in Geomechanics*, ed. C. S. Desai, I: 829-835, 2001.

[MAN 65] MANDEL J., "Une généralisation de la théorie de Koiter", *I. J. Solid Struct.*, 1, p. 273-295, 1965.

[MIT 82] MITCHELL J.K., MCMILLAN J.C., GREEN S.L. & SISSON R.C., "Thermal backfill materials", in *Underground Cable Thermal Backfill*, S.A. Boggs *et al.* Eds., Pergamon Press, New York, p. 19-33, 1982.

[MOD 92] MODARESSI H. & LALOUI L., "A cyclic thermoviscoplastic constitutive model for clays", *Numerical Models in Geomechanics - NUMOG IV*, vol. I, p. 125-134, 1992.

[MOD 94] MODARESSI H., LALOUI L. & AUBRY D., "Thermodynamical approach for Camclay-familly models with Roscoe-type dilatancy rules", *International journal for numerical and analytical methods in geomechanics*, vol. 18, p. 133-138, 1994.

[MOD 95] MODARESSI A. & MODARESSI H., "Thermoplastic constitutive model for unsaturated soils: A prospective approach", *Numerical Models in Geomechanics – NUMOG V.*, p. 45-50, 1995.

[MOD 97] MODARESSI H. & LALOUI L. "A thermo-viscoplastic constitutive model for clays", *Journal for Numerical and Analytical Methods in Geomechanics*, 21, p. 313-335, 1997.

[MOR 95] MORITZ L., "Geotechnical Properties of Clay at Elevated Temperatures", *Swedish Geotechnical Institute*, 69 p, 1995.

[NOB 69] NOBEL C.A. & ESRIG M.I., "Some temperature effects on strength behaviour of cohesive soil", *Highway Research Board*, Sp Rpt 103, p. 204-219, 1969.

[PER 63] PERZYNA, "The constitutive equations for rate sensitive plastic materials", *Quart. Appl. Math.*, 1963.

[PLU 69] PLUM R.L & ESRIG M.J, "Some temperature effects on soil compressibility and pore water pressure", *Highway Research Board*, Sp Rpt 103, p. 231-242, 1969.

[PRA 58] PRAGER W., "Non-isothermal plastic deformation", *Koninkklijk-Nederland Akademie Van Wetenschappen Te Amsterdam- Proceedings of the section of sciences- B.*, 61, 1958.

[ROB 96] ROBINET J.C., RAHBAOU A., PLAS F. & LEBON P., "A constitutive thermomechanical model for saturated clays", *Engineering Geology*, vol. 41, 1-4, p. 145-169, 1996.

[SCH 68] SCHOFIELD A.N. & WROTH C.P., *Criticat State Soil Mechanics*, McGraw-Hill, London, 1968.

[SVE 99] SVENDSEN B., HUTTER K. & LALOUI L., "Constitutive models for granular materials including quasi-static frictional behaviour: Toward a thermodynamic theory of plasticity", *Continuum Mechanics and thermodynamics*, vol. 11, Issue 4, p. 263-275, 1999.

[TID 89] TIDFORS M. & SÄLLFORS S., "Temperature effect on preconsolidation pressure", *Geotechnical testing Journal*, 12-1, p. 93-97, 1989.

[ZIE 75] ZIEGLER H., "Non-linearity in thermomechanics", *Int. J. Non-Linear Mech*., 10, p. 145-154, 1975.

[ZIE 77] ZIEGLER H., *An Introduction to Thermomechanics*, North-Holland, Amsterdam, 1977.

[ZIE 87] ZIEGLER H. & WEHRLI C., "The derivation of constitutive relations from the free energy and the dissipation function", *Advances in Applied Mechanics*, vol. 25, p. 183-257, 1987.